

SIMULATION OF RANDOM ELECTRON MULTIPLICATION IN CALIPSO LIDAR PHOTOMULTIPLIERS

Kathleen A. Powell⁽¹⁾, Zhaoyan Liu⁽²⁾, Bill Hunt⁽³⁾

⁽¹⁾*Science Applications International Corporation, MS 475, Hampton, VA, USA, 23681, k.a.powell@larc.nasa.gov*

⁽²⁾*National Institute of Aerospace, MS 475, Hampton, VA, USA, 23681, fn.z.liu@larc.nasa.gov*

⁽³⁾*Science Applications International Corporation, MS 475, Hampton, VA, USA, 23681, b.h.hunt@larc.nasa.gov*

ABSTRACT

CaliopSim is a high-fidelity lidar simulation [1] that has been developed to simulate the expected performance of the lidar named, Cloud-Aerosol Lidar with Orthogonal Polarization (CALIOP), on-board the Cloud-Aerosol Lidar and Infrared Pathfinder Satellite Observations (CALIPSO) spacecraft [2], [3]. The simulation tool is designed to generate realistic lidar data that models the CALIOP measurement data including the noise characteristics inherent to analog detection [4].

The detectors for CALIOP include photomultiplier tubes (PMT) for the 532 channels, and an avalanche photodiode (APD) for the 1064 channel. For each detector, the simulated distributions of the output electrons generated at the detector anode are based on processes that have a random element, which effectively produce the variations in secondary electron emission. For the PMT this process is modeled as a multiply stochastic Neyman type-A distribution [5] and the secondary electron emission for the APD is modeled as a combined Poisson and Gaussian probability distribution [6].

For CaliopSim, a direct implementation for the APD process was relatively straightforward and produced the expected excess noise. For the PMT, a direct implementation of the Neyman type-A process was not always possible because the simulated distributions of output electrons generated at later dynode stages are sensitive to the computer accuracy in representing floating point numbers. This paper describes an approach that was developed for CaliopSim that accurately represents the performance of the PMT.

1. INTRODUCTION

The CALIOP receiver subsystem measures backscatter intensity at 1064 nm and at two orthogonally polarized components of the 532 nm backscattered signal. The simulations for each detector consider four types of noise characteristics within the signal namely (a) photon noise, which is associated with the random arrival of the photons at the photocathode, (b) dark noise, the thermally sensitive noise present in

electronic devices in the absence of light, (c) circuit noise, which results from the thermal motion of charged carriers in resistors and amplifiers, and (d) excess noise, which is a result of the multiplication process [7].

For both detectors, the first three types of noise are modeled in a similar way. However, the internal multiplication process is not the same for the APD and PMT detectors and must be modeled separately by CaliopSim. However, the implementation of each multiplication process is identical. The steps include building the Probability Distribution Functions (PDFs), generating a Cumulative Distribution Function (CDF), and interrogating the CDF to generate a randomized gain amplified signal at the detector anode. While the PDFs for the APD simulation could be modeled accurately using a straight forward approach, the PDFs for the PMT simulation could not be.

This paper describes the implementation of the Neyman type-A process within CaliopSim. Results showing excess noise calculated from the simulated distributions of the output electrons are reported.

2. PMT SIMULATION

For CaliopSim, the PMT dynode chain electron emission is modeled as a multiply stochastic Neyman type-A distribution [5]. For each one electron generated at the photocathode, this model calculates the probabilities of obtaining k electrons at each node within the dynode chain having a Poisson-distributed secondary-emitting gain with mean m . The probability distribution function (PDF) describing this model is defined as

$$P_m(k_n) = \sum_{k_{n-1}=0}^{S_{\text{max}}} \left(p(k_{n-1}, m, k_n) \cdots \sum_{k_2=0}^{S_{\text{max}}} \left\{ p(k_2, m, k_3) \sum_{k_1=0}^{S_{\text{max}}} [p(k_1, m, k_2) p(k_0, m, k_1)] \right\} \right), \quad (1)$$

where the subscripts on the k variables refer to the dynode stage and

$$p(k_{n-1}m, k_n) = \frac{(k_{n-1}m)^{k_n} e^{-k_{n-1}m}}{k_n!}. \quad (2)$$

By setting k_0 equal to 1.0, the probability distribution $P_m(k_n)$ describes the probability of generating k_n electrons at dynode stage n for one incident electron at dynode stage 1. S_{mx} , the probability summation maximum, should approach infinity, but is limited by the precision of the software package or computer. For the CALIOP PMT, the number of dynode stages n is 13, and the multiplication factor, or mean dynode gain, m is 2.98595971 [8]. In CaliopSim, the value for S_{mx} is 249 and the electron numbers for each PDF range from 1.0 to $\mu_n + 6\sigma_n$. The mean μ_n and standard deviation σ_n of the PDFs at each stage are determined from the moment generating functions as defined by Liu [5].

The CDF, C_m , is defined as

$$C_m(x) = \frac{\sum_{i=0}^x P_m(i)}{C_m(x_{max})}, \quad x=0 \rightarrow x_{max} = \mu_{n=13} + 6\sigma_{n=13}, \quad (3)$$

where the x values define the number of electrons generated at the detector anode. $C_m(x)$ is normalized by the maximum value $C_m(x_{max})$. This step corrects for small errors that are introduced during $P_m(k_n)$ formulation and the discrete integration calculation. The CDF used for CALIOP simulations is computed using the dynode stage 13 PDF.

3. BUILDING DYNODE STAGE PDFs

The direct application of Eq. 1 requires building all dynode stage PDFs from stage 1 through n . This works well for modeling PMTs that have a small number of dynode stages and low mean dynode gains. However, as the number of dynode stages increase or the mean dynode gain is large, the direct application of Eq. 1 results in large inaccuracies in the computed PDFs. The problem occurs when the $k_n m$ terms become large, and the resulting exponential terms in the probability equations reach the lower limits of the computed floating point representation. S_{mx} is then defined as the maximum value of k_n for which the exponential term remains greater than 0.0.

An example in Fig. 1 shows PDFs computed by Eq. 1 for dynode stages 2 through 5. Valid PDF values (stages 2, 3, and first part of 4) correspond to electron numbers less than S_{mx} . Large errors are apparent in the stage 5 PDF for electron numbers greater than S_{mx} .

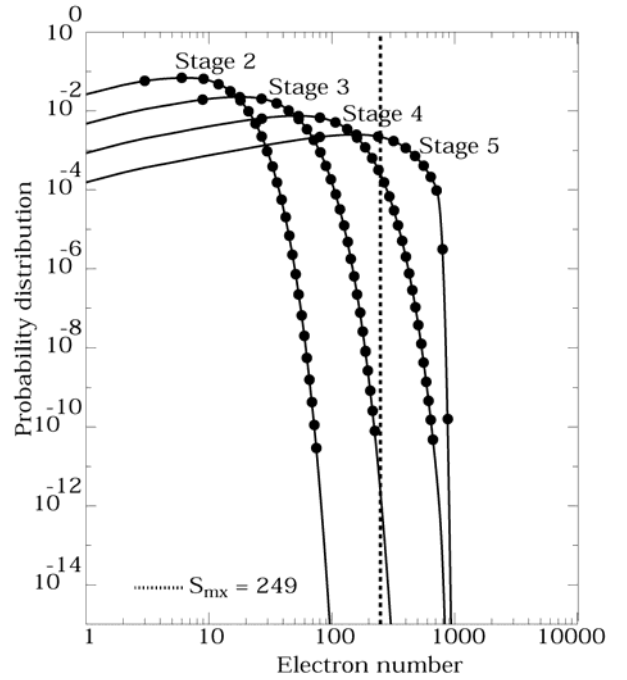


Fig. 1. PDFs for the CALIOP PMT dynode stages 2 through 5. The large dots on the PDF curves identify electron numbers through $\mu_n + 6\sigma_n$. The small dotted line coincides with $S_{mx} = 249$.

In order to calculate PDFs for the larger dynode stages, an alternate solution is required. A constant scale application described by Liu [5], transfers PDF values from early dynode stages (calculated by direct application) to corresponding PDF values at later dynodes stages using the mean dynode gain m as a constant scale factor. This technique performs well for electron numbers near the distribution mean values and for the largest dynode stages. However, for early and intermediate dynode stages, consecutive PDFs do not scale by a constant amount for electron numbers near the tails of the distributions. To show this, Fig. 2 contains three PDF ratio profiles, which were computed as the ratio of consecutive PDFs and plotted as functions of electron number. The PDF ratio values are approximately equal to m for electron numbers near the distribution means (labeled μ_2 , μ_3 , and μ_4), but monotonically decrease as electron numbers move away from the means.

To improve the accuracy of the constant scale application, CaliopSim includes an intermediate step between the direct application and the constant scale application. This intermediate step, named variable scale application, transfers PDF values from early dynode stages (calculated by direct application) to corresponding PDF values at later dynodes stages using a profile of variable scale factors.

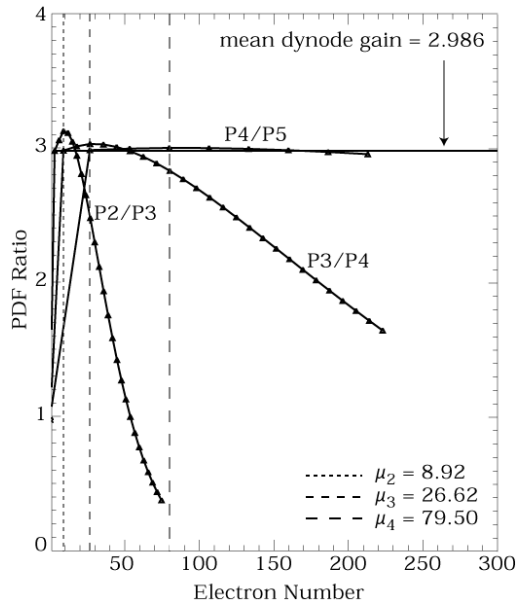


Fig. 2. Three PDF ratio profiles vs. electron number.

The three-step process is then performed as follows: the direct application is applied until the maximum number of electrons for the next PDF will exceed S_{mx} . Then the variable scale application is applied until it is determined that the ratio between the previous and the current PDF is nearly constant. The final PDFs are then computed using the constant scale application.

The variable scale PDF ratio profiles are extracted from a PDF ratio database for any number of dynode stages over a range of mean dynode gain values. For the CALIOP implementation, the ratio profile database is defined for 12 dynode stages (stages 2 through 13) and at 20 mean dynode gain values ranging from 1.2 to 3.1, with a 0.1 increment.

To show the improvement gained by including the variable scale application, the two approaches were compared. The first used only the constant scale application and the second used the combined variable and constant scale applications. PDFs from dynode stage 1 to 13 were generated for each approach. The dynode stage 13 PDFs were then used to build corresponding CDFs. The comparison study consisted of a series of 100 tests and each test included $1.0e6$ trial simulations. A trial simulation generates a random number of electrons at the detector anode for one electron emitted at the photocathode.

Following each test, the percent relative errors for both the means and standard deviations of the results from each approach were computed. For the constant scale application, the calculated percent relative errors for the standard deviation fluctuates about 0.8% and the percent relative errors for the mean fluctuates about 0.4%. Although, these percent relative errors are small,

improved results were obtained by adding the variable scale application. For the combined application, the calculated percent relative error for the standard deviation fluctuates about -0.05% and the percent relative error for the distribution mean fluctuates about -0.14%.

4. BUILDING PDF RATIO PROFILES

The PDF ratio profile database is constructed as follows. First, PDF ratio profiles for the selected number of dynode stages and mean dynode gains are computed using Eq. 1. Fig. 3 displays the plots of the PDF ratio profiles for the mean dynode gain, $m = 1.5$. This plot shows that early dynode stage ratio profiles are not constant, but later stage ratio profiles approach the constant value 1.5. Invalid ratio profile elements are eliminated before proceeding to the next step (indicated in the circled area in Fig. 3).

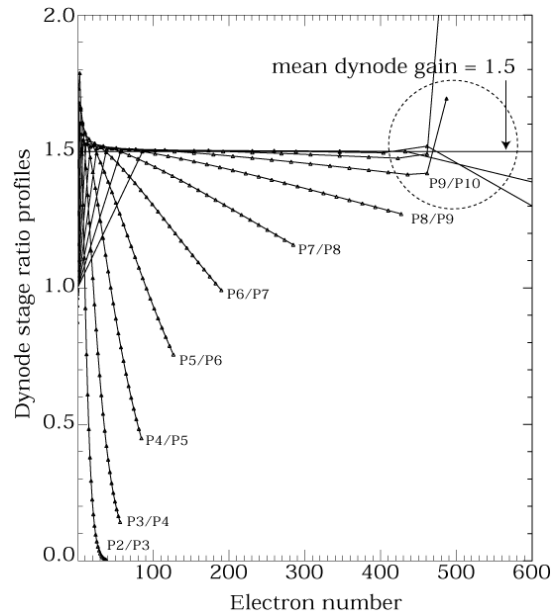


Fig. 3. PDF ratio profiles for mean dynode gain, 1.5.

Next, linear approximations of PDF ratios with electron number are applied and the resulting slope and y-intercept values are stored within their own databases. In Fig. 4, the stored slope database values vs. mean dynode gain are plotted as solid bold lines.

Linear approximations of the slope and y-intercept values (shown in bold) with the mean dynode gain values are computed and extrapolation (shown as dashed lines) is performed beyond the valid slope and y-intercept values.

To retrieve a PDF ratio profile for a selected dynode stage and mean dynode gain, the corresponding slope and y-intercept values are derived from the slope and

y-intercept databases. The derived slopes and y-intercepts are then used to reconstruct the PDF ratio profiles for the corresponding mean dynode gain value.

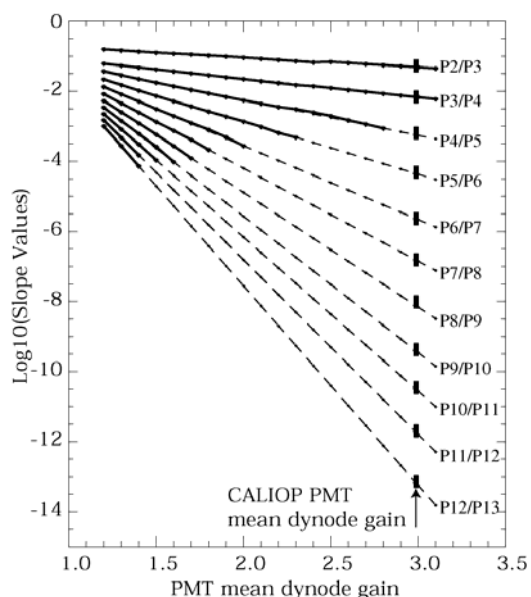


Fig. 4. Slope database values vs. mean dynode gain.

5. EXCESS NOISE CALCULATIONS

In the final analysis of the simulated results, the expected excess noise factor F_m [7] was compared to the computed results. The theoretical excess noise factor for the CALIOP PMT F_{PMT} is 1.23.

Excess noise factors for the PMT detector simulation were calculated by taking the ratios of two signal-to-noise ratios for molecular backscatter, a water cloud, and an ice cloud. The first set of signal-to-noise ratios were computed at the detector photocathode and the second set at the detector anode.

Excess noise calculations were generated for the 532 nm parallel and perpendicular signals that were simulated for both day and night conditions. The simulated data used in the excess noise calculations included the following 4 the regions: molecular backscatter at 2-4 km and 10-12 km; a water cloud at 2-4 km; and an ice cloud at 10-12 km.

The means for each horizontal resolution and at each region were computed and are listed in Table 1. The excess noise values for the simulated molecular profiles are low for the 5 km resolution. This is not unexpected since the number of photoelectrons generated at both the detector photocathode and anode are often very small values and would result in a low signal-to-noise ratio. The results obtained for the 20 km and 80 km resolutions agree well with the expected excess noise value.

Table 1. 532 nm excess noise calculations

	5.0 km		20.0 km		80.0 km	
	D	N	D	N	D	N
Molecular 2-4 km	1.20	1.11	1.22	1.20	1.22	1.22
Molecular 10-12 km	1.19	1.05	1.22	1.15	1.22	1.21
Ice Cloud 10-12 km Parallel	1.23	1.22	1.22	1.23	1.23	1.23
Ice Cloud 10-12 km Perpen.	1.22	1.17	1.22	1.22	1.22	1.22
Water Cloud 1-4 km	1.23	1.23	1.23	1.22	1.23	1.22

REFERENCES

1. K. A. Powell, The development of the CALIPSO lidar simulator, Master Thesis, The College of William and Mary, 2005.
2. D. M. Winker, J. R. Pelon, and M. P. McCormick, The CALIPSO mission: spaceborne lidar for observation of aerosols and clouds, *Proc. of SPIE*, 4893, pp. 1-11, 2003.
3. D. M. Winker., C. Hostetler, and W. Hunt, CALIOP: The CALIPSO Lidar, 22nd International Laser Radar Conference, Matera, Italy, 2004.
4. K. A. Powell, W. H. Hunt, D. M. Winker, Simulations of CALIPSO lidar data, 21st International Laser Radar Conference, L. Bissonnette, G. Roy, and G. Vallée, Eds, Québec, Canada, pp. 781-784, 2002.
5. Z. Liu and N. Sugimoto, Simulation study for cloud detection with space lidars by use of analog detection photomultiplier tubes, *Appl. Opt.*, 41, pp. 1750-1759, 2002.
6. P. P. Webb, R. J. McIntyre, and J. Conradi, Properties of Avalanche Photodiodes, *RCA Review*, 35, pp. 235-278, 1974.
7. Z. Liu, W. H. Hunt, C. A. Hostetler, M. A. Vaughan, M. McGill, K. A. Powell, D. M. Winker, and Y. Hu, Estimating random errors in backscatter lidar observations, submitted to *Appl. Opt.*, 2005.
8. W. Hunt, CALIPSO Lidar Receiver Electronics (LRE) Gains, NASA Systems Engineering Report WHH-030, June 2004.